Inorg. Chem. **2002**, *41*, 5091–5099

Octahedral (*cis*-Cyclam)iron(III) Complexes with *O*,*N*-Coordinated *o*-Iminosemiquinonate(1–) π Radicals and *o*-Imidophenolate(2–) Anions

Hyungphil Chun, Eckhard Bill, Eberhard Bothe, Thomas Weyhermüller, and Karl Wieghardt*

Max-Planck-Institut für Strahlenchemie, Stiftstrasse 34-36, D-45470 Mülheim an der Ruhr, Germany

Received May 8, 2002

Three octahedral complexes containing a (*cis*-cyclam)iron(III) moiety and an *O*,*N*-coordinated *o*-iminobenzosemiquinonate π radical anion have been synthesized and characterized by X-ray crystallography at 100 K: [Fe(*cis*-cyclam)(L_{1-3}^{ISQ})](PF_6)$_2$ (**1**–**3**), where (L_{1-3}^{ISQ}) represents the monoanionic π radicals derived from one-electron oxidations of the respective dianion of *o*-imidophenolate(2–), L_1, 2-imido-4,6-di-*tert*-butylphenolate(2–), L_2, and *N*-phenyl-2-imido-4,6-di-*tert*-butylphenolate(2–), L_3. Compounds **1**–**3** possess an $S_t = 0$ ground state, which is attained via strong intramolecular antiferromagnetic exchange coupling between a low-spin central ferric ion ($S_{Fe} = 1/2$) and an *o*-imino-benzosemiquinonate(1–) π radical ($S_{rad} = 1/2$). Zero-field Mössbauer spectra of **1**–**3** at 80 K confirm the low-spin ferric electron configuration: isomer shift $\delta = 0.26$ mm s^{-1} and quadrupole splitting $\Delta E_Q = 1.96$ mm s^{-1} for **1**, 0.28 and 1.93 for **2**, and 0.33 and 1.88 for **3**. All three complexes undergo a reversible, one-electron reduction of the coordinated *o*-imino-benzosemiquinonate ligand, yielding an [Fe^{III}(*cis*-cyclam)(L_{1-3}^{IP})]$^+$ monocation. The monocations of **1** and **2** display very similar rhombic signals in the X-band EPR spectra ($g =$ 2.15, 2.12, and 1.97), indicative of low-spin ferric species. In contast, the monocation of **3** contains a high-spin ferric center ($S_{Fe} = 5/2$) as is deduced from its Mössbauer and EPR spectra.

Introduction

In a series of papers,[1−6] we have recently shown that *O*,*N*-coordinated *o*-aminophenolates are redox noninnocent in the sense that they can be bound to a transition metal ion either as an *o*-imidophenolate dianion, $(L^{IP})^{2-}$, as shown in Scheme 1, or as an *o*-iminobenzosemiquinonate π radical anion, $(L^{ISQ})^{1-}$, or in principle, also as a neutral *o*-iminobenzoquinone ligand, $(L^{IBQ})^0$. We have not been able to synthesize and structurally characterize a coordination compound containing an *O*,*N*-coordinated *o*-iminobenzoquinone ligand but M(L^{ISQ}) and M(L^{IP}) species have been obtained and have been structurally characterized. The oxidation level of the ligand as aromatic in $(L^{IP})^{2-}$ or open shell in $(L^{ISQ})^{1-}$ is clearly discernible via low-temperature X-ray crystallography and other spectroscopies.[1−6]

A recent report by Vasconcellos et al.[7] caught our attention because these authors claim to have characterized the low-spin ferrous complex [Fe(*cis*-cyclam)(L_1^{IBQ})](PF_6)$_2$ by X-ray crystallography. Their structure report contains an inconsistency that indicated to us that their structure determination is seriously flawed. It is reported that the O—C bond length in (L_1^{IBQ}) at 1.335(10) Å is significantly longer than the corresponding N—C distance at 1.277(10) Å. This is in stark contrast to all structurally characterized *o*-aminophenolate complexes[1−6] where the O—C bond is always shorter than the N—C bond distance, regardless of the oxidation level of the ligand. Furthermore, their interpretation of the structural and other spectroscopic data and their conclusions regarding the oxidation level of the ligand and the oxidation state of the iron ions as L^{IBQ} and ferrous, respectively, appeared not to be in accord with our data, which include a detailed Mössbauer study. We decided to reinvestigate this compound

* To whom correspondence should be addressed. E-mail: wieghardt@mpi-muelheim.mpg.de.

(1) Verani, C. N.; Gallert, S.; Bill, E.; Weyhermüller, T.; Wieghardt, K.; Chaudhuri, P. *Chem. Commun*. **1999**, 1747−1748.
(2) Chaudhuri, P.; Verani, C. N.; Bill, E.; Bothe, E.; Weyhermüller, T.; Wieghardt, K. *J. Am. Chem. Soc*. **2001**, *123*, 2213−2223.
(3) Chun, H.; Verani, C. N.; Chaudhuri, P.; Bothe, E.; Bill, E.; Weyhermüller, T.; Wieghardt, K. *Inorg. Chem*. **2001**, *40*, 4157−4166.
(4) Chun, H.; Weyhermüller, T.; Bill, E.; Wieghardt, K. *Angew. Chem., Int. Ed*. **2001**, *40*, 2489−2492.
(5) Chun, H.; Chaudhuri, P.; Weyhermüller, T.; Wieghardt, K. *Inorg. Chem*. **2002**, *41*, 790−795.
(6) Sun, X.; Chun, H.; Hildenbrand, K.; Bothe, E.; Weyhermüller, T.; Neese, F.; Wieghardt, K. *Inorg. Chem*. **2002**, *41*, 4295.
(7) Vasconcellos, L. C. G.; Oliveira, C. P.; Castellano, E. E.; Ellena, J.; Moreira, I. S. *Polyhedron* **2000**, *20*, 493−499.

10.1021/ic020329g CCC: $22.00
Published on Web 09/12/2002

Scheme 1

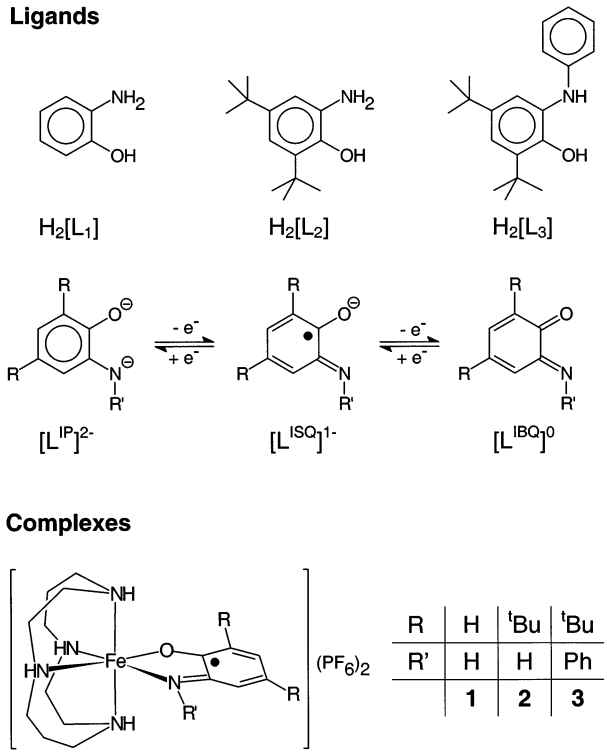

1. In addition, we synthesized two closely related complexes, **2** and **3**, containing the ligands L_2 and L_3 shown in Scheme 1.

The diamagnetic ground state of complexes **1**, **2**, and **3** (Scheme 1) is conclusively and unambiguously shown to be generated from a strong intramolecular antiferromagnetic coupling between a low-spin ferric ion (d,[5] $S_{Fe} = 1/2$) and an *O*,*N*-coordinated $(L_{1-3}{}^{ISQ})^-$ π radical anion. In addition, we have also investigated the electronic structure of the corresponding one-electron reduced monocations [Fe(*cis*-cyclam)$(L_{1-3}{}^{IP})]^+$ in solution.

Experimental Section

1,4,8,11-Tetraazacyclotetradecane (cyclam), 2-aminophenol, and potassium tetrathionate were obtained commercially. 2-Amino-4,6-di-*tert*-butylphenol[8] and 2-anilino-4,6-di-*tert*-butylphenol[2] were prepared according to published methods. *cis*-[Fe(cyclam)Cl_2]Cl was prepared by reacting equimolar amounts of ferric chloride and cyclam in ethanol or methanol at room temperature.[9]

[Fe(*cis*-cyclam)$(L_1{}^{ISQ})](PF_6)_2$ (1). A methanolic solution (10 mL) of [Fe(cyclam)Cl_2]Cl (110 mg, 0.3 mmol), 2-aminophenol (33 mg, 0.3 mmol), and triethylamine (0.1 mL) was stirred under an argon atmosphere at room temperature for 3 h. After ammonium hexafluorophosphate (150 mg, 0.9 mmol) was added, the solution was exposed to air with continued stirring for 1 h and then filtered. A dark blue solid residue obtained after the filtrate had dried was redissolved in 5 mL of an acetonitrile−water mixture (4:1) and the resulting solution was allowed to evaporate slowly by passing an argon stream over the solution, which yielded a dark blue-black crystalline precipitate (150 mg, 76%). Single crystals suitable for X-ray structure analysis were selected from the crystalline product. Anal. Calcd for $C_{16}H_{29}N_5OP_2F_{12}Fe$ (653.21 g mol^{-1}): C, 29.42; H, 4.47; N, 10.72. Found: C, 29.48; H, 4.41; N, 10.82%. ESI-MS (CH_3CN, positive ion): m/z = 508 $\{M - PF_6\}^+$, 182 $\{M - 2PF_6\}^{2+}$, 128 $\{M - 2PF_6 - C_6H_5NO\}^{2+}$ (100%).

[Fe(*cis*-cyclam)$(L_2{}^{ISQ})](PF_6)_2$ (2). Compound **2** was obtained by following the same procedure as described above for **1** using 2-amino-4,6-di-*tert*-butylphenol instead of 2-aminophenol in 61% yield. The crude product (blue powder) was recrystallized by liquid diffusion of diethyl ether into a concentrated solution of **2** in methanol. Anal. Calcd for $C_{24}H_{45}N_5OP_2F_{12}Fe$ (765.43 g mol^{-1}): C, 37.66; H, 5.93; N, 9.15. Found: C, 37.88; H, 5.93; N, 9.04%. ESI-MS (CH_3OH, positive ion): m/z = 620 $\{M - PF_6\}^+$, 238 $\{M - 2PF_6\}^{2+}$ (100%).

[Fe(*cis*-cyclam)$(L_2{}^{ISQ})]S_4O_6 \cdot 2H_2O$ (2a). The cation of **2** was also isolated as a tetrathionate salt from the reaction mixture by adding 1 equiv of potassium tetrathionate dissolved in a minimum amount of water at the end of the reaction. After a white precipitate was filtered off, the filtrate was allowed to stand at ambient temperature, yielding a crystalline blue-black precipitate (78% yield). Single crystals selected from the precipitate were used for X-ray diffraction study. Anal. Calcd for $C_{24}H_{49}N_5O_9S_4Fe$ (735.77 g mol^{-1}): C, 39.18; H, 6.71; N, 9.52. Found: C, 39.56; H, 6.38; N, 9.52%. ESI-MS (CH_3CN, positive): m/z = 238 $\{M - S_4O_6 - 2H_2O\}^{2+}$ (100%).

[Fe(*cis*-cyclam)$(L_3{}^{ISQ})](PF_6)_2$ (3). [Fe(cyclam)Cl_2]Cl (260 mg, 0.7 mmol), triethylamine (0.4 mL), and 2-anilino-4,6-di-*tert*-butylphenol (210 mg, 0.7 mmol) were dissolved in 25 mL of absolute ethanol. The solution was stirred at room temperature under an argon atmosphere until it had dried. The resulting dark purple solid residue was redissolved in absolute ethanol (10 mL), and after ammonium hexafluorophosphate (470 mg, 2.9 mmol) was added, the solution was stirred for 1 h in the presence of air. A dark purple-blue precipitate was collected by filtration, washed with water (10 mL) and ethanol (2 mL), and dried in vacuo at 70 °C (280 mg, 46%). Single crystals for an X-ray structure determination were obtained by slow evaporation of the solution of **3** in a mixture of ethanol/acetone/water (10:5:1) under an argon atmosphere for 2 weeks. Anal. Calcd for $C_{30}H_{49}N_5OP_2F_{12}Fe$ (841.53 g mol^{-1}): C, 42.82; H, 5.87; N, 8.32. Found: C, 42.56; H, 5.84; N, 8.08%. ESI-MS (CH_3CN, positive ion): m/z = 696 $\{M - PF_6\}^+$, 275 $\{M - 2PF_6\}^{2+}$ (100%).

Physical Measurements. The electronic spectra of the complexes and spectra of the spectroelectrochemcial investigations were recorded on an HP 8453 diode array spectrophotometer (range 190−1100 nm). Cyclic voltammetry and coulometric experiments were performed using an EG&G potentiostat/galvanostat. Temperature-dependent (2−298 K) magnetization data were recorded on a SQUID magnetometer (MPMS Quantum design) in an external magnetic field of 1.0 T. The experimental susceptibility data were corrected for underlying diamagnetism by the use of tabulated Pascal's constants. X-band EPR spectra were recorded on a Bruker ESP 300E spectrometer equipped with a helium flow cryostat (Oxford Instruments ESR 910), an NMR field probe (Bruker 035M), and a microwave frequency counter HP5352B. Spin-Hamiltonian simulations of the EPR spectra were preformed with a program that was developed from the routines of Gaffney and Silverstone[10] and that specifically makes use of the resonance-search procedure based on a Newton−Raphson algorithm as described therein. Frequency- and angular-dependent contributions to the line widths were considered in the powder simulations. The line shape of the

(8) Stegmann, H. B.; Scheffler, K. *Chem. Ber.* **1968**, *101*, 262−271.
(9) Chan, P. K.; Poon, C.-K. *J. Chem. Soc., Dalton Trans.* **1976**, 858−862.
(10) Gaffney, B. J.; Silverstone, H. J. In *EMR of Paramagnetic Molecules*; Berliner, L. J., Reuben, J., Eds.; Plenum Press: New York, 1993; Vol. 13.

Table 1. Summary of Crystallographic Data Collection and Structure Refinements of **1**−**3**

	1	**2a**	**3**
empirical formula	$C_{16}H_{29}N_5OP_2F_{12}Fe$	$C_{24}H_{45}N_5O_7S_4Fe\cdot1.3H_2O$	$C_{30}H_{49}N_5OP_2F_{12}Fe$
FW	653.23	723.16	841.53
cryst syst	monoclinic	monoclinic	triclinic
space group	$P2_1/n$	$P2_1/c$	$P\bar{1}$
a (Å)	9.1945(6)	11.2677(8)	9.5149(9)
b (Å)	15.8491(9)	12.7849(10)	9.8258(9)
c (Å)	17.3321(12)	24.173(2)	21.244(2)
α (deg)	90	90	78.37(1)
β (deg)	103.90(1)	100.37(1)	87.67(1)
γ (deg)	90	90	69.01(1)
V (Å^3)	2451.8(3)	3425.4(5)	1815.2(3)
Z	4	4	2
T (K)	100 (2)	100 (2)	100 (2)
D_{calc} (g cm^{-3})	1.770	1.402	1.540
μ (mm^{-1})	0.858	0.735	0.599
F(000)	1328	1532	872
cryst size (mm)	0.16 × 0.12 × 0.12	0.25 × 0.15 × 0.15	0.24 × 0.24 × 0.06
T_{max}/T_{min}	0.917/0.871	0.959/0.844	0.965/0.851
total reflns/$2\theta_{max}$ (deg)	18339/62	22982/55	13763/55
unique [R(int)]	7783 (0.0549)	7781 (0.0601)	8093 (0.0997)
observed [$I > 2\sigma(I)$]	5180	5661	6027
data/parameters	7732/337	7711/403	8047/0/460
GOF	1.033	1.042	1.061
R1, wR2 [$I > 2\sigma(I)$]	0.0515, 0.1124	0.0462, 0.0881	0.0680, 0.1593
R1, wR2 (all data)	0.0933, 0.1363	0.0772, 0.1006	0.0968, 0.1792
ρ_{max}/ρ_{min} (e Å^{-3})	0.718/−0.472	0.350/−0.372	0.989/−0.624

spin packets were either Lorentzian or Gaussian. The simulations are based on the spin Hamiltonian for the electronic spin ground-state multiplet:

$$H = D[S_z^2 - S(S+1)/3 + (E/D)(S_x^2 - S_y^2)] + \mu_B B\cdot g\cdot S$$

where S is the total spin multiplet (5/2) and D and E/D are the usual axial and rhombic zero-field parameters. Distributions of E/D (or alternatively D) were taken into account by summation of a series of powder spectra calculated at distinct values of that parameter with weight factors taken from the Gaussian distribution. The distributed parameter was equidistantly sampled in the range ±3 times the width of the Gaussian distribution and usually 50 EPR spectra were superimposed in this procedure. The intrinsic width of the spin packets (Gaussian line shape) was taken to be at least 10 mT (at $g = 2$). NMR experiments were carried out on a Bruker ARX spectrometer (400 MHz). The ^{57}Fe Mössbauer spectra were measured on an Oxford Instruments Mössbauer spectrometer in zero field. ^{57}Co/Rh was used as a radiation source. The temperature of the sample was controlled by an Oxford Instruments Variox Cryostat. Isomer shifts were determined relative to α-iron at 300 K. The minimum experimental line width was 0.24 mm s^{-1}.

X-ray Crystallographic Data Collection and Refinement of the Structures. Single crystals of **1**, **2a**, and **3** were fixed with perfluoropolyether on glass fibers and mounted on a Nonius Kappa-CCD diffractometer equipped with a cryogenic nitrogen cold stream operating at 100(2) K. Graphite monochromated Mo Kα radiation (λ = 0.710 73 Å) was used. Intensity data were corrected for Lorentz and polarization effects. The intensity data set of **2a** was corrected for absorption using the program MulScanAbs embedded in the PLATON99 program suite.[11] The crystal faces of **1** and **3** were determined and the face-indexed correction routine embedded in SHELXTL[12] was used to account for absorption. The Siemens SHELXTL[12] software package was used for solution and refinements of the structures. All structures were solved and refined by direct methods and difference Fourier techniques. Non-hydrogen atoms were refined anisotropically. Hydrogen atoms at N(22) in **1** and **2a** and of one water molecule in **2a** were readily located from difference maps and their positional parameters were refined independently. The oxygen atom of the second water molecule in the structure of **2a** was partially occupied (30%) and left without hydrogen atoms. Details of the data collection and structure refinements are summarized in Table 1, and selected bond distances and angles are given in Table 2.

Table 2. Selected Bond Distances (Å) and Angles (deg)

	1	**2a**	**3**
Fe(1)−N(1)	2.029(2)	2.026(2)	2.027(3)
Fe(1)−N(4)	2.020(2)	2.006(2)	2.028(3)
Fe(1)−N(8)	2.044(2)	2.057(2)	2.060(3)
Fe(1)−N(11)	2.018(2)	2.003(2)	2.025(3)
Fe(1)−N(22)	1.864(2)	1.865(2)	1.920(3)
Fe(1)−O(21)	1.917(2)	1.906(2)	1.892(2)
O(21)−C(21)	1.300(3)	1.301(3)	1.299(4)
N(22)−C(22)	1.326(4)	1.334(3)	1.350(4)
C(21)−C(22)	1.440(4)	1.438(3)	1.445(5)
C(22)−C(23)	1.428(4)	1.426(3)	1.416(5)
C(23)−C(24)	1.358(4)	1.365(4)	1.365(5)
C(24)−C(25)	1.426(5)	1.437(4)	1.442(5)
C(25)−C(26)	1.358(4)	1.370(4)	1.380(5)
C(21)−C(26)	1.415(4)	1.429(4)	1.434(4)
N(1)−Fe(1)−O(21)	174.33(9)	177.05(8)	176.79(13)
N(4)−Fe(1)−N(11)	171.63(9)	169.72(9)	169.58(13)
N(8)−Fe(1)−N(22)	169.49(10)	168.11(9)	167.92(12)
N(1)−Fe(1)−N(4)	84.17(9)	84.36(9)	83.32(14)
N(1)−Fe(1)−N(8)	97.18(9)	96.68(8)	95.90(14)
N(1)−Fe(1−-N(11)	90.98(10)	88.99(9)	89.91(14)
N(4)−Fe(1)−N(8)	89.81(9)	88.75(9)	89.44(14)
N(8)−Fe(1)−N(11)	84.02(9)	84.23(8)	83.36(13)

Results and Discussion

Synthesis. The ligand 2-amino-4,6-di-*tert*-butylphenol H_2-[L_2] prepared via a condensation reaction of 3,5-di-*tert*-butylcatechol and aqueous ammonia, followed by reduction with sodium borohydride, was first reported in 1968.[8] The EPR spectrum of its one-electron air-oxidized form, the deep

(11) Spek, A. L. University of Utrecht, The Netherlands, 1999.
(12) *SHELXTL*, V. 5; Siemens Analytical X-ray Instruments, Inc.: Madison, WI, 1994.

blue π radical $(L_2^{ISQ})^{-\bullet}$ has been reported at that time. Subsequently, its synthesis via the reduction of 3,5-di-*tert*-butyl-2-nitrophenol[13] or by a deamination reaction of ethylenediamine with 3,5-di-*tert*-butylbenzoquinone[14] has been reported. The crystal structure of $H_2[L_2]$ was described.[14] The solution of $H_2[L_2]$ is highly air-sensitive. The synthesis of the ligand 2-anilino-4,6-di-*tert*-butylphenol, $H_2[L_3]$, via condensation of 3,5-di-*tert*-butylcatechol with aniline has been described.[2]

Octahedral complexes **1**, **2**, and **3** containing a (*cis*-cyclam)iron(III) moiety and an *O*,*N*-coordinated *o*-imino-benzosemiquinonate π radical anion, $(L_{1-3}^{ISQ})^{1-}$, have been isolated as bis(hexafluorophosphate) salts or, in the case of **2**, also as tetrathionate salt **2a**. The compounds were obtained from the reaction mixture of *cis*-$[Fe^{III}(cyclam)Cl_2]Cl$, the corresponding *o*-aminophenol and triethylamine in methanol or ethanol, which were stirred at 20 °C first in the absence of air under an argon blanketing atmosphere and then in the presence of air. After addition of $[NH_4]PF_6$, dark blue, slightly hygroscopic powders of $[Fe(cis\text{-cyclam})(L_{1-3}^{ISQ})](PF_6)_2$, **1**−**3**, were obtained in good yields.

Upon repeated recrystallizations of **1**, a brownish precipitate was obtained whose IR spectrum did not show the bands of coordinated 2-aminophenolate. Compound **2** seems to be robust toward repeated dissolution and evaporation. However, its high solubility in all common solvents was the major problem in obtaining single crystals for a structural study. The crystals of **2** obtained by slow evaporation of acetonitrile solution or by liquid diffusion of diethyl ether into the methanol solution were flaky. When we tried to isolate the cation of **2** with a tetrathionate anion, a conformationally flexible dianion with better hydrogen-bonding capability than hexafluorophosphate, single crystals of **2a** with well-defined morphology and adequate sizes for single-crystal X-ray crystallography were obtained. Spectroscopic measurements were carried out for both the hexafluorophosphate and the tetrathionate salt. Compound **3** was recrystallized under anaerobic conditions, and single crystals suitable for X-ray analysis were obtained as thin plates. Finally, we note that the analytical, spectroscopic, and crystallographic data for compound **1** are the same as those reported by Vasconcellos et al.,[7] ruling out the possibility that we have prepared a valence isomer of the original compound.

Complexes **1**, **2**, and **3** are diamagnetic as was judged from their normal ^{1}H NMR spectra recorded at ambient temperature. An exemplary spectrum of **1** is shown in Figure 1. The fact that these complexes all possess an $S = 0$ ground state was also established by temperature-dependent magnetic susceptibility measurements (SQUID; 2−298 K) in an external magnetic field of 1 T (not shown). As we will show conclusively below, the $S = 0$ ground state in **1**, **2**, and **3** is attained via strong intramolecular, antiferromagnetic exchange coupling between a low-spin ferric ion ($S_{Fe} = 1/2$) and an *o*-imino-benzosemiquinonate π radical ($S_{rad} = 1/2$).

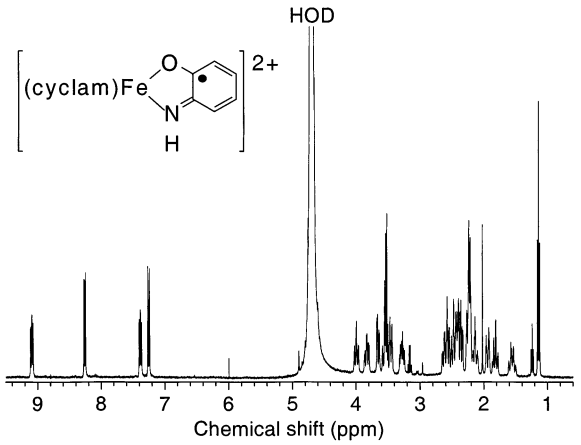

Figure 1. ^{1}H NMR spectrum of **1** in D_2O at room temperature.

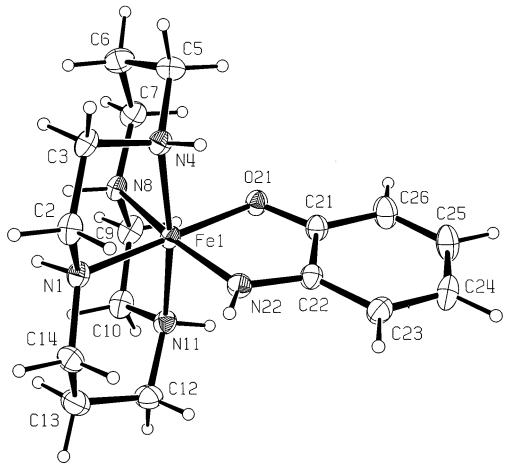

Figure 2. ORTEP[23] view of the cation of **1** shown at 50% probability level. Hydrogen atoms are drawn as open circles of arbitrary size.

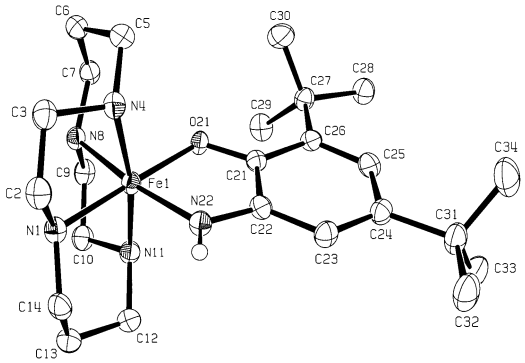

Figure 3. Structure of the cation of **2a** shown at 50% probability level. All the hydrogen atoms except for that of N22 have been omitted for clarity.

Crystal Structures. The results of the X-ray structure determinations of **1**, **2a**, and **3** are shown in Figures 2, 3, and 4, respectively. Crystallographic data are given in Table 1, while selected bond lengths and angles are presented in Table 2. The crystal structures have been determined at 100(2) K to minimize the estimated standard deviations as compared to the reported room-temperature structure of **1**. It was also hoped that it would be possible to unambiguously locate the imine hydrogen atoms of the *O*,*N*-coordinated

(13) Fukata, G.; Sakamoto, N.; Tashiro, M. *J. Chem. Soc., Perkin Trans. 1* **1982**, 2841−2848.
(14) Jimenez-Perez, V. M.; Camacho-Camacho, C.; Güizado-Rodriguez, M.; Nöth, H.; Contreras, R. *J. Organomet. Chem.* **2000**, *614*−*615*, 283−293.

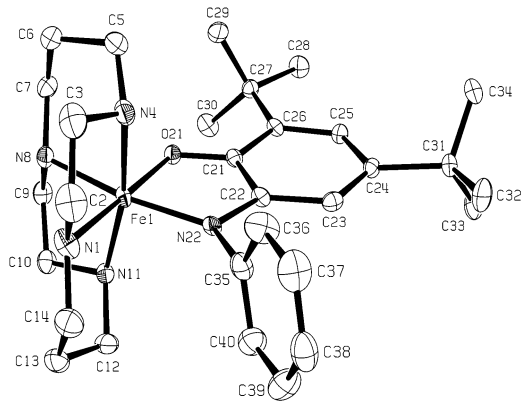

Figure 4. Perspective view of the cation of **3** shown at 40% probability level. Hydrogen atoms have been omitted for the sake of clarity.

ligands in **1** and **2a** in the final difference Fourier syntheses. Note that in the previous structure determination at 293(2) K this hydrogen atom had probably not been experimentally located but was "stereochemically positioned".[7] This procedure led to an incorrect assignment of oxygen and nitrogen donor atoms of the aminophenolate moiety which, as we will show, must be inverted.

The geometrical features of the (*cis*-cyclam)Fe moiety of all three structures are very similar and are in excellent agreement with many other structure determinations of complexes containing this unit. It is stressed that the positions of the amine protons of the coordinated *cis*-cyclam ligand have been located unambiguously in the final difference Fourier maps in all three structures. The Fe—N_{amine} bond distances in **1**, **2a**, and **3** are observed in the range 2.003(2)−2.060(3) Å, which indicates the presence of a low-spin ferric (or ferrous) central ion[15−17] because for the corresponding high-spin ions the Fe—N_{amine} distances are observed in the range 2.15−2.21 Å.[15,16] A similar pattern is found for the Fe—N and Fe—O bond lengths of the *O*,*N*-coordinated *o*-aminophenolate derivatives in **1**, **2a**, and **3**. These bond distances are short at ∼1.90 Å for the Fe—O bond and at 1.87 Å for the Fe—N bonds in **1** and **2a**. They are 1.89 (±0.01) and 1.92 (±0.01) Å, respectively, for **3**. In high-spin $[Fe^{III}(L_3^{ISQ})_3]$ the average Fe—O length is at 2.01, and the average Fe—N bond distance is 2.10 Å.[3]

In the following we develop a consistent scheme that allows one to discern among the three resonance structures A, B, and C in Scheme 2 by X-ray crystallography. Thus, the oxidation level of a given *O*,*N*-coordinated *o*-aminophenolate derivative is readily identified by the following structural features (Scheme 2): (i) the C—O bond distance decreases from 1.35 Å in $(L^{IP})^{2-}$ ligands to 1.30 Å in $(L^{ISQ})^{-\bullet}$ and probably <1.30 Å in $(L^{IBQ})^0$; (ii) concomitantly the C—N bond length decreases from 1.37 Å in $(L^{IP})^{2-}$ to 1.35 Å in $(L^{ISQ})^{-\bullet}$ and to (probably) 1.32 Å in $(L^{IBQ})^0$; (iii) the six C—C bonds in $(L^{IP})^{2-}$ are equidistant at ∼1.405 Å; the six-membered ring is aromatic; in $(L^{ISQ})^{1-\bullet}$ a quinoid-type distortion of this ring is observed with two alternating short C—C bonds at 1.375 Å and four longer ones at ∼1.43 Å; for $(L^{IBQ})^0$ this distortion is expected to be even more pronounced.

Scheme 2

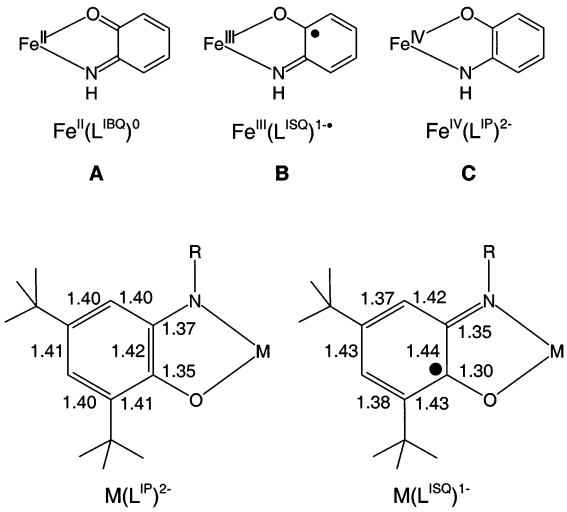

Complex **2a** contains a 2-imino-4,6-di-*tert*-butylbenzosemiquinonate π radical where the imino group is readily and unambiguously identified by X-ray crystallography. The two *tert*-butyl groups in 4,6 positions render the oxygen and nitrogen positions unique and not interchangeable as in **1**. It is therefore significant at the 3σ level that the C—O bond is shorter than the C—N bond at 1.301(3) and 1.334(3) Å, respectively. It is significant—even at the 3σ confidence level—that the Fe—O distance at 1.906(2) Å is longer than the Fe—N_{amine} bond length at 1.865(2) Å. Gratifyingly, the same holds true for our structure of **1** in which we have located the imino hydrogen atom in the final difference Fourier map in the vicinity of the atom N22 and no residual electron density is found near O21. The observed C—O, C—N, and C—C distances of the *O*,*N*-coordinated *o*-imino-benzosemiquinonates in **1** and **2a** reflect clearly the benzosemiquinonate oxidation level because their geometrical features are identical to those reported for a series of other coordination compounds containing *o*-imino-benzosemiquinonato(1−) radicals.[1−6]

Similarly, the structure of **3** clearly shows the presence of an *O*,*N*-coordinated *o*-imino-benzosemiquinonate(1−) anion. These results necessitate the presence of low-spin ferric ions in **1**, **2**, and **3** and are not compatible with the notion of Vasconcellos et al.[7] that the dication in crystals of **1** contains a low-spin ferrous ion coordinated to a neutral cyclam and a neutral *o*-imino-benzoquinone ligand.

Electro- and Spectroelectrochemistry. Figure 5 displays the electronic spectra of complexes **1**, **2**, and **3** in acetonitrile solution at ambient temperature. They are deep blue in solution and in the solid state. The spectra are very similar and display two very intense absorption maxima ($\epsilon \sim 6 \times 10^3$ M^{-1} cm^{-1}) in the range 500−700 nm. Interestingly, both λ_{max} values shift bathochromically from 607 to 633 and to 658 nm on going from **1** to **2** and to **3** (Table 3) and similarly

(15) Guilard, R.; Siri, O.; Tabard, A.; Broeker, G.; Richard, P.; Nurco, D. J.; Smith, K. M. *J. Chem. Soc., Dalton Trans.* **1997**, 3459−3463.
(16) Meyer, K.; Bill, E.; Mienert, B.; Weyhermüller, T.; Wieghardt, K. *J. Am. Chem. Soc.* **1999**, *121*, 4859−4876.
(17) Ballester, L.; Gutierrez, A.; Perpinan, M. F.; Rico, S.; Azcondo, M. T.; Bellitto, C. *Inorg. Chem.* **1999**, *38*, 4430−4434.

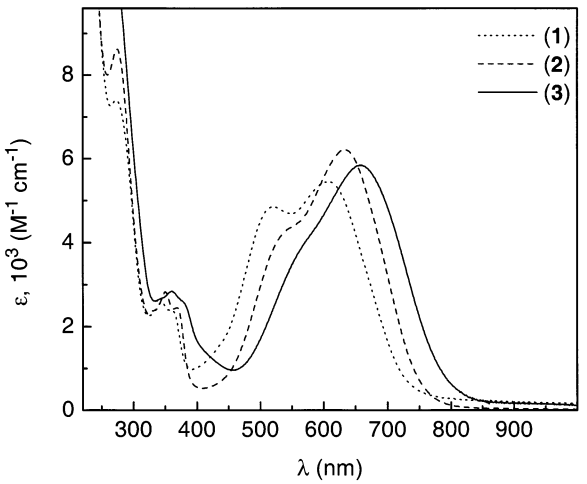

Figure 5. Electronic absorption spectra of **1**−**3** measured in acetonitrile solution at room temperature.

Table 3. Electronic Spectra of Complexes in CH_3CN at 20 °C

complex	λ_{max}, nm (ϵ, M^{-1} cm^{-1})
1	280 (7.2×10^3), 344 (2.6×10^3), 520 (4.9×10^3), 607 (5.5×10^3)
reduced **1**[a]	298 (5.8×10^3), 371 (3.0×10^3), 485 (2.6×10^3), 815 (4.3×10^3)
2	275 (8.6×10^3), 350 (2.9×10^3), 370 (2.5×10^3), 540 sh, 633 (6.2×10^3)
reduced **2**[a]	281 (11.8×10^3), 364 (2.8×10^3), 523 (2.5×10^3), 852 (4.1×10^3)
3	360 (2.8×10^3), 380 sh, 570 sh, 658 (5.8×10^3)
reduced **3**[a]	380 sh, 554 (3.3×10^3), 883 (3.9×10^3)

[a] Electrochemically generated monocation.

Table 4. Redox Potentials of Complexes (CH_3CN; 0.10 M $[TBA]PF_6$; Glassy Carbon Working Electrode; $Ag/AgNO_3$ Reference Electrode; 200 mV s^{-1} Scan Rate, 20 °C)

complex	$E_{1/2}^1$, V[a]	$E_{1/2}^2$, V[a]
1	0.82	−0.63
2	0.73	−0.71
3	0.80	−0.42

[a] In volts vs Fc^+/Fc.

from 520 to 540 and to 570 nm. The spectrum of Krüger et al.'s complex $[Fe^{III}(L-N_4Me_2)(dbsq)]^{2+}$ is quite similar.[18] This intense absorption has been tentatively assigned by the authors as an LMCT transition of the *O*,*O*-coordinated semiquinonate, $(dbsq)^{-\bullet}$.

The electrochemical activity of **1**−**3** has been studied by cyclic voltammetry in CH_3CN containing 0.10 M $[TBA]PF_6$ as a supporting electrolyte. All redox potentials are referenced vs the ferrocenium/ferrocene, Fc^+/Fc, couple. The results are summarized in Table 4, and Figure 6 shows the cyclic voltammograms of **1**, **2**, and **3** recorded in the potential range 1.1 to −1.0 V. Each compound displays two reversible one-electron-transfer waves. Upon expansion of the potential range scanned to −1.6 V, a third highly irreversible wave is observed at approximately −1.4 V, which was not investigated in any further detail. This process is expected to be a metal-centered reduction ($Fe^{III} \rightarrow Fe^{II}$). Controlled-potential coulometry established that the reversible waves at negative

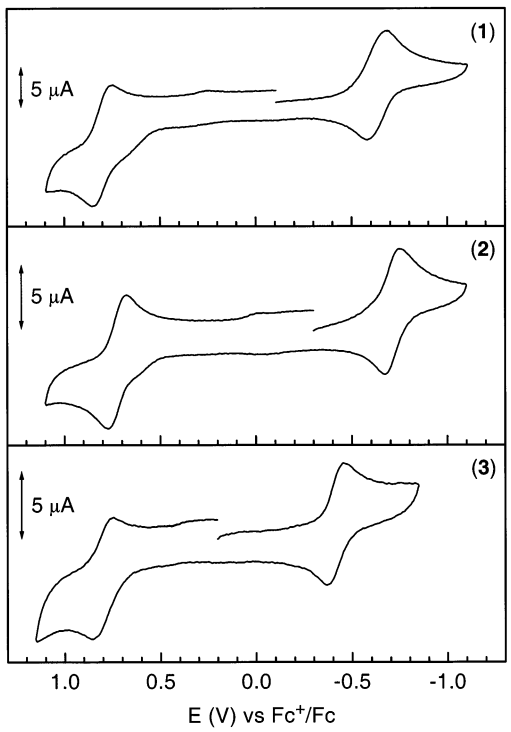

Figure 6. Cyclic voltammograms of **1** (top), **2** (middle), and **3** (bottom) measured in acetonitrile solution at room temperature. For measurement conditions, see Table 4.

potentials correspond to a one-electron reduction of **1**, **2**, and **3**, respectively, yielding a monocation. The corresponding waves at positive potentials are one-electron oxidation processes yielding tricationic species. The oxidized forms of **1**, **2**, and **3** were found to not be stable on the time scale of coulometric experiments and have, therefore, not been studied. Thus, the electrochemistry of **1**−**3** follows the pattern shown in eq 1, where the first two one-electron reductions

$$[(\text{cyclam})Fe^{III}(L^{IBQ})]^{3+} \underset{-e^-}{\overset{+e^-}{\rightleftharpoons}} [(\text{cyclam})Fe^{III}(L^{ISQ})]^{2+} \underset{-e^-}{\overset{+e^-}{\rightleftharpoons}} [(\text{cyclam})Fe^{III}(L^{IP})]^{+} \xrightarrow{+e^-} [(\text{cyclam})Fe^{II}(L^{IP})]^{0} \xrightarrow{\text{fast}} \text{decomposition products} \quad (1)$$

are ligand-centered and the third irreversible process is metal-centered. Vasconcellos et al.[7] reported a differential pulse voltammogram of **1** dissolved in an aqueous buffer at pH = 3 and found three sequential one-electron transfer waves. It is not possible to compare their measured redox potentials meaningfully with ours due to the presence of protons in their solution which enables coupled proton-/electron-transfer processes. Figure 7 shows the changes observed during the electrochemical one-electron reduction of **1**, **2**, and **3** in CH_3CN solution (0.10 M $[TBA]PF_6$) at 20 °C. In each reduction a number of clear isosbestic points are observed. Interestingly, the resulting spectra of the monocations of **1**−**3** are very similar; each exhibits two absorption maxima at ∼520 and ∼850 nm (Table 3). These monocations of **1**−**3** are quite stable in anaerobic acetonitrile solution. Electrochemical reoxidation of such solutions produced quantitatively the spectra of the starting materials.

Because **1**−**3** are diamagnetic species, their one-electron reduced forms should be paramagnetic. Therefore, we have

(18) Koch, W. O.; Schünemann, V.; Gerdan, M.; Trautwein, A. X.; Krüger, H.-J. *Chem. Eur. J.* **1998**, *4*, 1255−1265.

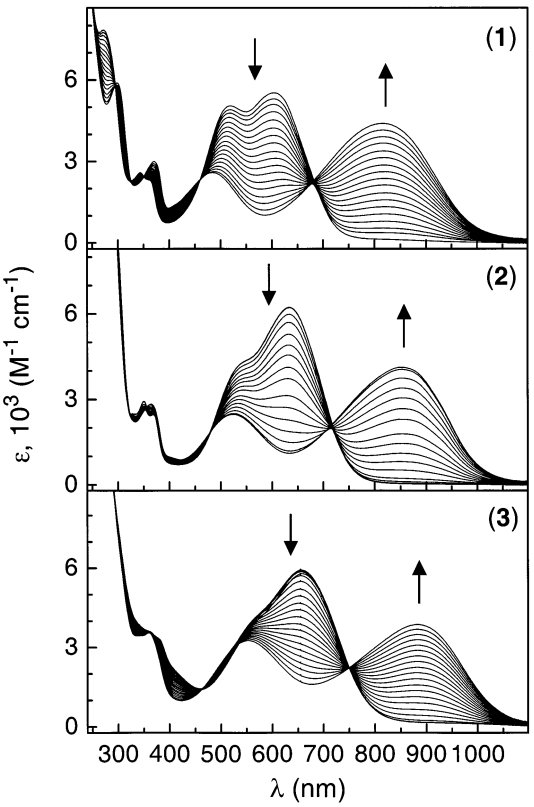

Figure 7. The change of absorption spectra during the electrochemical one-elecron reduction of **1** (top), **2** (middle), and **3** (bottom) at room temperature in acetonitrile solution containing 0.1 M $[N(n\text{-}Bu)_4]PF_6$.

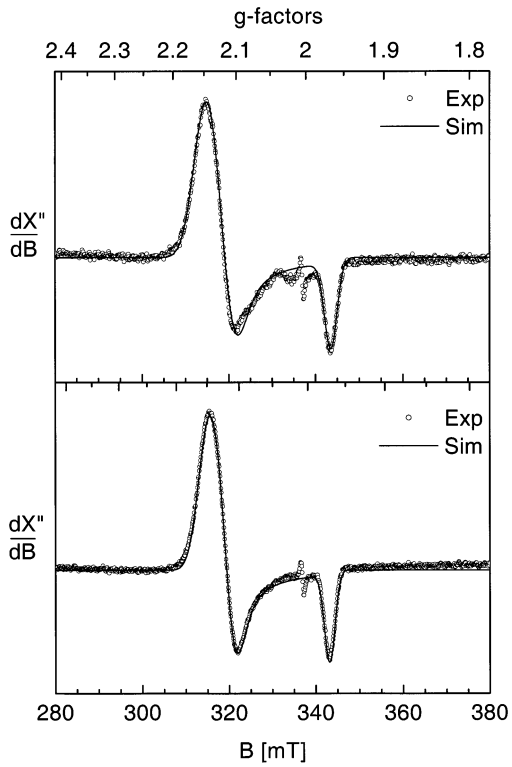

Figure 8. Experimental and simulated X-band EPR spectra of **1** (top) and **2** (middle) measured after electrochemical one-electron reduction in acetonitrile solution. Concentration: 0.7 mM for **1** and 0.5 mM for **2**. Frequency: 9.457 GHz for **1** and 9.456 GHz for **2**. Power: 0.01 mW for **1** and 0.02 mW for **2**. Modulation amplitude: 10 G for both. Temperature: 3.0 K for both.

measured X-band EPR spectra of CH_3CN solutions of electrochemically one-electron-reduced **1** and **2** at 3 K and **3** at 10 K. Figure 8 shows the spectra of the monocations of **1** and **2**, respectively. Clearly, an axial $S = 1/2$ signal with a slight rhombic distortion is observed for both species. From simulations the following g values were obtained for reduced **1** and reduced **2**, $g = 2.15$, 2.12, and 1.97. The very weak additional signal at $g = 2.0$ is possibly due to a small amount of free *o*-imino-benzosemiquinonate radical. Thus, monocations of **1** and **2** possess an $S = 1/2$ ground state and the unpaired electron predominantly resides in a metal d orbital. Thus, they contain a low-spin ferric ion with an *O*,*N*-coordinated, aromatic *o*-imidophenolato(2−) dianion. In other words, the one-electron reduction of **1** and **2** is a ligand-centered process, and the iron(III) ions retain their low-spin configuration during the reduction.

We expected a similar X-band EPR spectrum for the one-electron-reduced form of **3** because its spectroscopic and electrochemical features reported so far are nearly identical to those of **1** and **2**. To our surprise, we did not observe an $S = 1/2$ signal for reduced **3** in acetonitrile, but obtained the spectrum shown in Figure 9. The narrow isotropic signal at $g = 2.0$ again indicates the presence of uncoordinated *o*-imino-benzosemiquinonate radical in a trace amount (<1% integrated intensity). The spectrum of reduced **3** is dominated by two distinct low-field signals at $g = 9$ and $g = 5.3$ that are typical of high spin $S = 5/2$ with large zero-field splitting ($D \gg h\nu$). From a rhombogram that presents the effective g values of well-separated Kramers doublets as a function of rhombicity E/D,[19] the signals can be assigned to the $g_y(1)$ and $g_z(2)$ powder transitions of the Kramers doublets (1) and (2) as they are depicted in the top inset of Figure 9. The rhombicity parameter E/D obtained in such way is about 0.17. The powder lines of doublets (1) and (2) for the other principal directions different from *y* and *z*, respectively, are then expected as shown by the simulated trace "sub" at the top of the figure. Kramers doublet (3) is virtually EPR silent at $E/D = 0.17$ because of large g anisotropy and related low transition probabilities. However, instead of a number of resolved powder lines, the experimental spectrum shows only an unresolved derivative line at $g = 3.4$ and a trough at $g \sim 2.3$ with drastically increasing broadening with field. Nevertheless, the spectrum can be well-simulated with $S = 5/2$ if only a Gaussian distribution of the rhombicity parameter is adopted with half width $\sigma(E/D) = 0.02$ (trace "sim"). We assume that structural microheterogeneity of the solvated molecules in the frozen acetonitrile matrix is responsible for the heterogeneity of the rhombicity. The Gaussian shape of the distribution is taken for convenience and is based on the assumption of statistically arbitrary perturbations of the ligand field symmetry. The optimized values of the other spin-Hamiltonian parameters are $D = 3.01(\pm 0.5)$ cm^{-1}, $E/D = 0.166(\pm 0.005)$, $g = 2$ (fixed), and frequency-dependent Gaussian line width $w_f = 2$ mT (at $g = 2$).

(19) Trautwein, A. X.; Bill, E.; Bominaar, E. L.; Winkler, H. *Struct. Bonding* (*Berlin*) **1991**, *78*, 1−95.

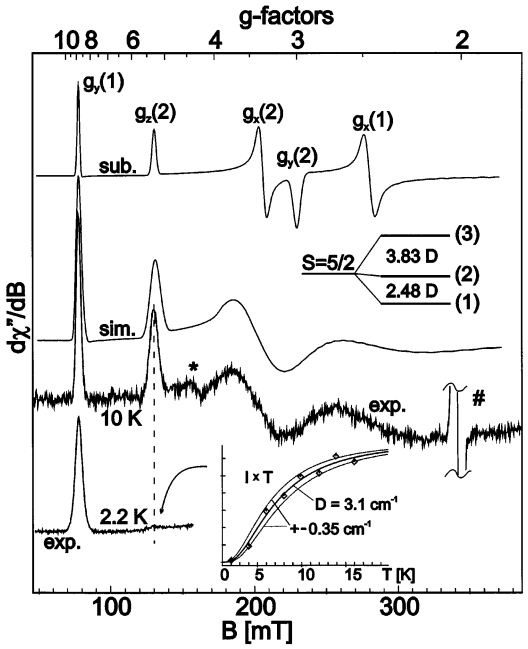

Figure 9. X-band EPR spectra of **3** measured after electrochemical one-electron reduction in acetonitrile solution (0.5 mM) at 2 and 10 K, and spin Hamiltonian simulation at 10 K. Asterisk (*) denotes an impurity from traces of nuisance Fe(III). Residual radical signal is cut (#). Experimental conditions: frequency, 9.6353 GHz; power, 10 μW; modualtion amplitude, 1 mT/100 kHz. Simulation (trace "sim") for $S = 5/2$ with spin Hamiltonian parameters $D = 3.01$ cm^{-1}, $E/D = 0.166$, frequency-dependent Gaussian line width $w_f = 2$ mT, and Gaussian distribution of E/D with $\sigma(E/D) = 0.02$. Trace "sub" is the center subspectrum of the distribution with the same parameters without $\sigma(E/D)$. The *middle inset* shows a diagram of the $S = 5/2$ manifold with the Kramers doublets (1)...(3) and their ZFS 2.48 and 3.83 D. The *bottom inset* shows the intensity of the $g_z(2)$ resonance times temperature vs temperature and the solid and dotted lines are Boltzmann functions $I \times T = \exp\{-2.48D/kT\}/(1 + \exp\{-2.48D/kT\} + \exp\{-6.31D\})$ with D values as indicated.

Compound **3** is one of the rare examples of an iron(III) high-spin compound with large axial ZFS so that D and E/D can be determined from a single X-band EPR measurement. Usually, hexacoordinated Fe(III) sites show rather small D ($\lesssim 1$ cm^{-1}) and most of them are fully rhombic, $E/D \sim 0.33$, unless a strong equatorial or axial ligand like a porphyrin or another macrocycle induces large axial ZFS.[20,21] "Finite" values of E/D far from the limiting cases $E/D = 0$ and 1/3 are rather unusual. For the reduced compound **3** the rhombicity $E/D = 0.17$ yields resolved lines from two different Kramers doublets, and D is of the order kT at liquid helium temperatures. Therefore, D is readily determined from one spectrum by the relative intensities of $g_y(1)$ and $g_z(2)$ transitions. For compound **3** the temperature variations of the line intensities are quite significant in the range 2−20 K, as indicated by the 2 K measurement shown at the bottom of Figure 9. The D value obtained from the simulation of the 10 K data was corroborated by recording thermal population/depopulation of the resonance levels for $g_y(1)$ and $g_z(2)$. The top inset of the figure shows the corresponding line intensities of $g_z(2)$ for the first excited doublet as a function of "intensity × temperature" vs temperature together with the corresponding Boltzmann function. A fit yields $D = 3.1(\pm 0.35)$ cm^{-1}, consistent with the simulation result.

Bearing the similarity of the electronic spectra of **1**−**3** and of their respective mono-reduced forms in mind, we are convinced that the reduction is also ligand-centered in **3**. However, unlike **1** and **2**, the iron ion in **3** appears to change its spin state from low spin in the dication to high spin in the monocation. This is confirmed by Mössbauer spectroscopy (see below).

Table 5. Zero-Field Mössbauer Parameters of Complexes

complex	T, K	δ,[a] mm s^{-1}	ΔE_Q,[b] mm s^{-1}	S_{Fe}[c]	S_t[d]	ref
$[Fe^{III}(L^{ISQ})_3]$	80	0.54	1.03	5/2	1	3
$[Fe^{III}(L-N_4Me_2)(dbsq)](ClO_4)_2$	4.2	0.18	2.32	1/2	0	17
trans-$[Fe^{III}(cyclam)(N_3)_2]ClO_4$	80	0.28	2.24	1/2	1/2	15
cis-$[Fe^{III}(cyclam)(N_3)_2]ClO_4$	80	0.49	0.26	5/2	5/2	15
trans-$[Fe^{II}(cyclam)(N_3)_2]$	80	0.55	0.72	0	0	15
cis-$[Fe^{II}(cyclam)(N_3)_2]$	80	1.11	2.84	2	2	15
cis-$[Fe^{III}(cyclam)Cl_2]Cl$	80	0.44	0.20	5/2	5/2	22
1	80	0.26	1.96	1/2	0	this work
2	80	0.28	1.93	1/2	0	this work
3	80	0.33	1.88	1/2	0	this work
reduced **1**[e]	200	0.23	1.91	1/2	1/2	this work
reduced **2**[e]	80	0.25	1.79	1/2	1/2	this work
reduced **3**[f]	80	0.46	1.12	5/2	5/2	this work

[a] Isomer shift vs α-Fe at 20 °C. [b] Quadrupole splitting. [c] Local spin state at iron ion. [d] Ground state. [e] Electrochemically generated monocation in CH_3CN (0.10 M $[TBA]PF_6$) using ^{57}Fe-labeled starting material. [f] Chemically reduced from **3**.

Mössbauer Spectroscopy. Zero-field Mössbauer spectra of solid samples of complexes **1**−**3** have been recorded at 80 K; the results are summarized in Table 5. Figure 10 shows the spectra of **1** and **3**, along with their mono-reduced forms. The spectrum of **2** is very similar to that of **1** and not shown. Each complex displays a single quadrupole doublet with very similar isomer shift, δ, and quadrupole splitting, ΔE_Q, parameters. The isomer shift is relatively low whereas the quadrupole splitting is rather large. These parameters unequivocally indicate the presence of a low-spin ferric ion in **1**−**3** ($S_{Fe} = 1/2$), as is deduced from the similarity of these parameters with those observed for *trans*-$[Fe^{III}(cyclam)(N_3)_2]ClO_4$ ($S_t = 1/2$) and Krüger et al.'s complex $[Fe^{III}(L-N_4Me_2)(dbsq)](ClO_4)_2$ ($S_t = 0$; $S_{Fe} = 1/2$),[18] where (dbsq) represents the 3,5-di-*tert*-butylbenzosemiquinonate(1−) radical.

If **1** would have the electronic structure $[Fe^{II}(cyclam)(L_1^{IBQ})]^{2+}$ containing a low-spin ferrous ion and a neutral, diamagnetic *o*-iminobenzoquinone ligand, as suggested by Vasconcellos et al.,[7] its Mössbauer parameters would be expected to be $\delta \sim 0.5$ mm s^{-1} and $\Delta E_Q \sim 0.7$ mm s^{-1} like those reported for diamagnetic *trans*-$[Fe^{II}(cyclam)(N_3)_2]$.[16]

The zero-field Mössbauer spectra of electrochemically generated, reduced **1** and **2** have been recorded in frozen CH_3CN solution (0.10 M $[TBA]PF_6$) at 80 K using ^{57}Fe labeled starting materials; the one-electron reduced form of **3** was obtained by chemical reduction of **3** with cobaltocene, and its spectrum was measured for a solid sample at 80 K. The Mössbauer parameters obtained for reduced **1** and **2** have changed little compared to their starting compounds and are

(20) Bencini, A.; Gatteschi, D. *Transition Metal Chemistry*; Melson G. A., Figgis, B. N., Eds.; Marcel Dekker: New York, 1982; Vol. 8, p 1.
(21) Neese, F.; Solomon, E. I. *Inorg. Chem.* **1998**, *37*, 6568−6582.
(22) Locally measured.
(23) Burnett, M.; Johnson, C. *ORTEP*−*III*; Report ORNL-6895; Oak Ridge National Laboratory, Oak Ridge, TN, 1996.

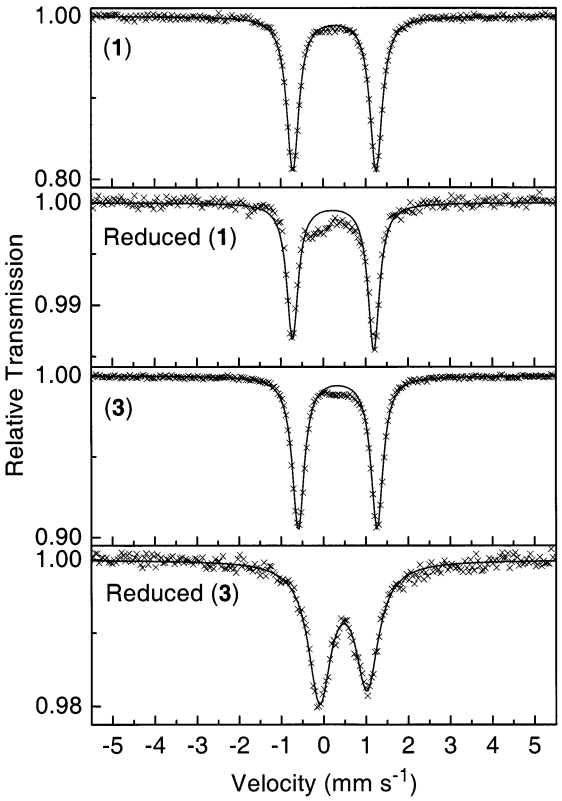

Figure 10. Zero-field Mössbauer spectra of **1** and **3** and their mono-reduced species. Solid lines represent the best fits. For measurement conditions, see Table 5.

in accordance with the presence of a low-spin ferric ion, rendering the one-electron reduction of **1** and **2** ligand-centered. In contrast, reduced **3** displays a higher isomer shift at 0.46 mm s^{-1}, which is in full agreement with a high-spin ferric ion.

Conclusion

This study reveals that the reaction of *cis*-[Fe^{III}(cyclam)-Cl_2]Cl with an *o*-aminophenol derivative, ($H_2[L_{1-3}]$), in the presence of triethylamine and dioxygen yields diamagnetic complexes [Fe^{III}(*cis*-cyclam)(L_{1-3}^{ISQ})](PF_6)$_2$, **1**−**3**. From structural and spectroscopic data it has been conclusively and unambiguously deduced that their electronic structure must be described as octahedral low-spin ferric species containing an *O*,*N*-coordinated *o*-imino-benzosemiquinonate-(1−) π radical ($[L_{1-3}^{ISQ}]^{1-}$). Strong intramolecular antiferromagnetic coupling between these two entities yields the observed diamagnetic ground state for **1**−**3**. The alternative formulation[7] as low-spin ferrous bound to a diamagnetic *o*-imino-benzoquinone is not in accordance with the structural and/or spectroscopic data. One-electron reduction of the dications [Fe^{III}(*cis*-cyclam)(L_{1-3}^{ISQ})]$^{2+}$ is shown to be a ligand-centered process yielding monocations [Fe^{III}(*cis*-cyclam)(L_{1-3}^{IP})]$^{+}$ where the ferric ion is low spin in reduced **1** and **2**, but high spin in reduced **3**.

Acknowledgment. We thank the Fonds der Chemischen Industrie of Germany for financial support. H. Chun is grateful for a fellowship from the Alexander von Humboldt Foundation.

Supporting Information Available: Complete listings of atomic coordinates, bond lengths and bond angles, anisotropic thermal parameters, and calculated positional parameters of hydrogen atoms for complexes **1**, **2a**, and **3**. This material is available free of charge via the Internet at http://pubs.acs.org.

IC020329G